# Generation of High-Power Broad-Band Microwave Pulses by Picosecond Optoelectronic Technique

HRAYR A. SAYADIAN, MEMBER, IEEE, M. G. LI, AND CHI H. LEE, SENIOR MEMBER, IEEE

*Abstract*—**A single-picosecond GaAs photoconductive switch (PS) is used to pulse excite a microwave resonant cavity, thus generating a variety of RF waveforms with picosecond synchronization. The length of the transmission line that connects the photoconductive switch and the cavity, and the strength of input/output cavity coupling elements provide for continuous variation of the frequency distribution of the generated RF power. The generation of over 7 kW, the peak-to-peak voltage over 1.2 kV, of broad-band microwave bursts is demonstrated.**

## I. INTRODUCTION

IN THE LAST few years, there has been great interest in the generation of coherent microwave pulses using ultrashort optical pulses [1]–[7]. These techniques use optical pulses to trigger photoconductive switches, thus allowing picosecond synchronization of the generated microwave pulses. Mourou *et al.* [1] used an optoelectronic switch, within a coaxial line connected to an *X*-band waveguide, to drive an *X*-band dish-type antenna. They also improved this technique by generating short pulses in a coaxial line system that fed a Hertzian dipole antenna [2]. Heidemann *et al.* demonstrated the generation of microwave pulses by optically triggering a photoconductive switch holding dc voltage across a tapered slot-line antenna [3]. More recently, DeFonzo *et al.* used a similar scheme to generate and detect millimeter waves [4]. Mooradian generated microwave radiation, from optoelectronic switches, by spatial time-division multiplication of the repetition rate of mode-locked laser pulses [5]. In our laboratory, Chang *et al.* demonstrated the generation of high-voltage sequential waveforms using the concept of frozen wave generation [6], and Sayadian *et al.* demonstrated the generation, multiplication, and shaping of ultrashort variable-width high-voltage pulses [7]. The latter work utilized parallel charging and series discharging methods, and used two photoconductive switches only (one GaAs and one Si) to generate and continuously shape nano/picosecond electrical pulses with over 100 kW of output peak power.

In general, it is desirable to use a small number of photoconductive switches in obtaining the highest voltages, so as not to overtask the triggering optical pulses. Earlier, we demonstrated conversion of dc energy to single-frequency RF energy, albeit at low voltage and power, using a single photoconductive switch and a coaxial resonant cavity [8]. In this paper we demonstrate the versatility of this technique. Among the different RF waveforms generated, we have produced broad-band microwave pulses with over 7 kW of peak power.

In Section II, we present theoretical considerations concerning photoconductive switches. Section III describes the experimental system used. Discussion of the results is given in Section IV. Conclusions are presented in Section V. In the Appendix we develop general relationships between the frequency distribution of the power for monopolar, dipolar, and multiplexed dipolar pulses.

## II. THEORETICAL CONSIDERATIONS

The field of photoconductive switching was created when Cr:GaAs was used to observe nanopicosecond laser pulses [9], and Si was used to switch, gate, and sample voltage pulses in a microstrip line [10]. Over the course of a decade, various workers have shown the immense applicability of picosecond photoconductive switches [11].

In Fig. 1 we show the schematic of the elemental photoconductive switch (PS) and the equivalent electrical circuit. The gap capacitance $C_g$ is due to the fringing fields associated with the discontinuity in the electrode (i.e., the gap). The value of $C_g$ is of the order of 50 fF [12]. $G(t)$ is the dynamic conductance of the PS and can be written as $G(t) = G_{\text{dark}} + g(t)$, where $G_{\text{dark}}$ is the dark conductance and $g(t)$ is the conductance due to the photogenerated carriers (generally $g(t) \gg G_{\text{dark}}$). The on-resistance of the PS is given [13] by

$$R_{\text{on}} = l^2 E_\lambda / [e\mu E_L (1-r)]$$

where $l$ is the length of the PS, $E_\lambda$ is the energy of a single photon, $E_L$ is the energy of the laser pulses, $\mu$ is the electrical mobility of the carriers, and $r$ is the optical reflectance of the PS material. The laser pulse energy

Manuscript received October 4, 1987; revised July 19, 1988. This work was supported in part by the Air Force Office of Scientific Research and the Army Research Office.

H. A. Sayadian was with the Department of Electrical Engineering, University of Maryland. He is now with the TRW Corporation, Redondo Beach, CA 90278.

M. G. Li and C. H. Lee are with the Department of Electrical Engineering, University of Maryland, College Park, MD 20742.

IEEE Log Number 8824257.

0018-9480/89/0100-0043$01.00 ©1989 IEEE

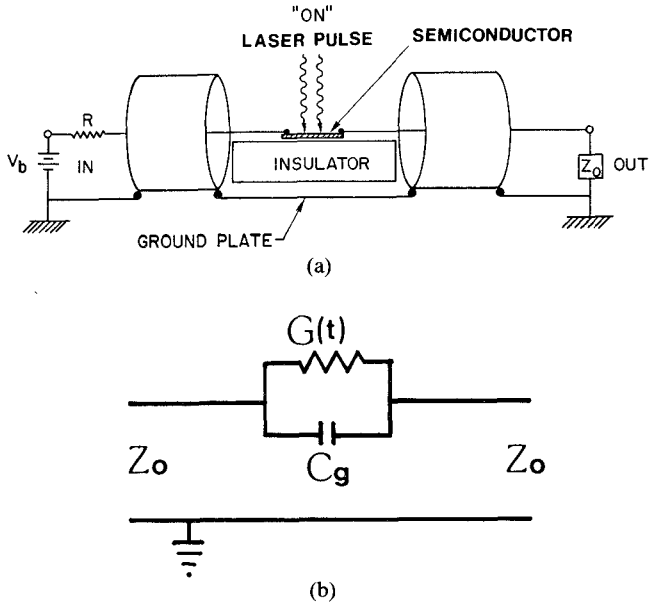


Fig. 1. (a) Schematic of the elemental photoconductive switch arrangement. (b) Equivalent circuit of (a).

required to achieve $R_{on} \simeq 1\ \Omega$, for 1 mm of PS gap length, is of the order of 2 $\mu$J for GaAs and 10 $\mu$J for Si. The difference between GaAs and Si stems from the difference in their carrier mobility. Note that $R_{on}$ depends on the square of the gap length, and that the width and thickness of the PS do not affect $R_{on}$.

The ultimate speed of response of the PS is limited by the dielectric relaxation time (femtoseconds) of the photogenerated carriers. However, the presence of gaps causes a much slower response time. The combination of $C_g$, $G(t)$, and $Z_0$ results in a charging circuit configuration which will degrade the rise time of electrical pulses that are triggered by the laser pulses. This effect can be seen by considering the idealized case of a step function $G(t)$:

$$G(t) = \begin{cases} 0, & t < 0 \\ G_1, & t \geqslant 0. \end{cases}$$

The output voltage is then given by [14],

$$V_{out} = \frac{V_b}{2} \cdot \frac{2Z_0G_1}{1+2Z_0G_1} \cdot \left[1 - \exp\left(-t/R_{eq}C_g\right)\right] \quad (1)$$

where

$$\frac{1}{R_{eq}} = \frac{1}{2Z_0} + G_1.$$

[Equation (1) shows that two different regimes of PS operation exist; namely $Z_0G_1 \ll 1$ and $Z_0G_1 \gg 1$. If $Z_0G_1 \ll 1$, then the rise time of the electrical pulse is $2Z_0C_g$ (usually several picoseconds) and the magnitude of $V_{out}$ is $Z_0G_1V_b$. This case is used in generating picosecond electrical pulses, through the use of very low mobility PS, albeit at very low-voltage output efficiency. If $Z_0G_1 \gg 1$, then the rise time is $C_g/G_1$ (subpicoseconds), and the magnitude of $V_{out}$ saturates at $V_b/2$.

The second case, $Z_0G_1 \gg 1$, is the regime in which high-voltage generating PS work. Note that in this case the limitation of $C_g/G_1$ on the rise time reduces with increasing $G_1$. In realistic situations, the PS is triggered by a laser pulse with a rise time of $\gtrsim 10$ ps. Since the rise time of the electrical circuit is a fraction of a picosecond, the electrical rise time follows the optical rise time. The electrical fall time, on the other hand, depends on the recombination time of the photogenerated carriers. In the absence of further optical excitation, carrier recombination causes the carrier density to reduce. Consequently, $G_1(t)$ reduces in time to $G_{dark}$. The reduction in the carrier density is given by $n(t) = n_0e^{-t/t_{rec}}$, where $t_{rec}$ is the carrier recombination time. Hence, $G_1(t) \propto e^{-t/t_{rec}}$. Equation (1) was obtained for constant $G_1$. However, if we are to consider slow variations ($t_{rec} \gg 2Z_0C_g/1+2Z_0G_1$ is true in general for significant $V_{out}$) then $V_{out} = V_b/2(2Z_0G_1/1+2Z_0G_1)$. Note that transients associated with $C_g$ will disappear well before $G_1$ changes in any significant amount. As $G_1(t)$ decreases, the PS operation will pass from the first case to $Z_0G_1 \simeq 1$ and then $Z_0G_1 \ll 1$, where $V_{out} \propto G_1(t) \propto e^{-t/t_{rec}}$. This asserts the remark about the fall time of electrical pulses.

The rise and fall times of electrical pulses have important consequences on the frequency distribution of the power. If we approximate the generated electrical pulses by

$$V(t) = \begin{cases} V_0\exp\left(t/t_r'\right), & t < 0 \\ V_0\exp\left(-t/t_f'\right), & t \geqslant 0 \end{cases}$$

where $t_r' \ll t_f'$, and $t_r', t_f'$ denote the rise and fall times, respectively, then

$$|V(\omega)| = V_0 \frac{\left(1+t_r'/t_f'\right)}{\left[\left(1/t_f' + \omega^2 t_r'\right)^2 + \omega^2\left(1 - t_r'/t_f'\right)^2\right]^{1/2}}$$

$$\simeq \frac{V_0}{\left[\left(1/t_f' + \omega^2 t_r'\right)^2 + \omega^2\right]^{1/2}}.$$

In Fig. 2 we show $|V(\omega)|$ as a function of $\omega$ for different $t_f'$, when $t_r' = 0$. Note the significant difference at low frequencies, while high-frequency components are the same. In Fig. 3 we show $|V(\omega)|$ for different $t_r'$, and $t_f' = 0.2$ ns. In this case the high-frequency components differ significantly, with the shorter rise-time pulse having higher frequency components. Hence, shorter rise-time optical trigger pulses generate high-frequency microwaves more efficiently.

The two materials most widely used as high-voltage (HV) PS are GaAs and Si. GaAs has a high dark resistivity, hence it is not prone to thermal runaway due to HV dc bias. However, photogenerated carriers recombine in about $\sim 5$ ns in pure GaAs, and in $\sim 200$ ps in Cr:GaAs. Consequently, GaAs is not ideal for the generation of pulses longer than $\sim 5$ ns. Workers have utilized the HV dc holding capability of GaAs and had to cope with its disadvantage [15]. Si, on the other hand, is ideal for microsecond electrical pulse generation and shaping be-

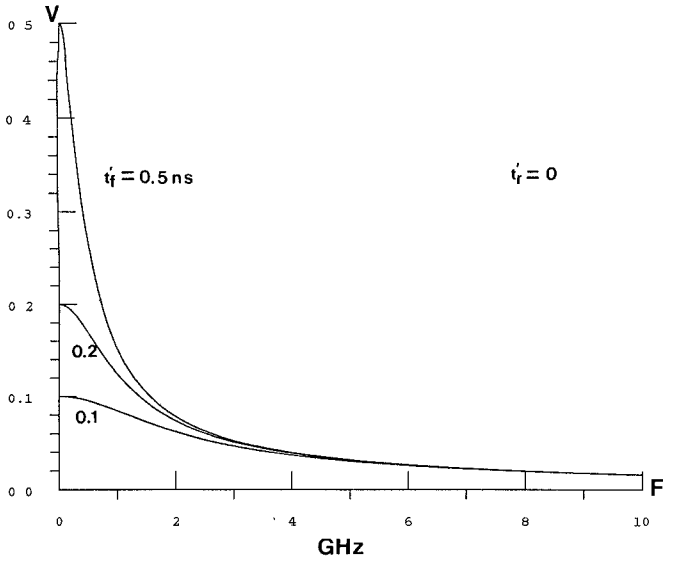


Fig. 2. $|V(\omega)|$ versus $\omega$ for different $t_f'$, $t_r' = 0$.

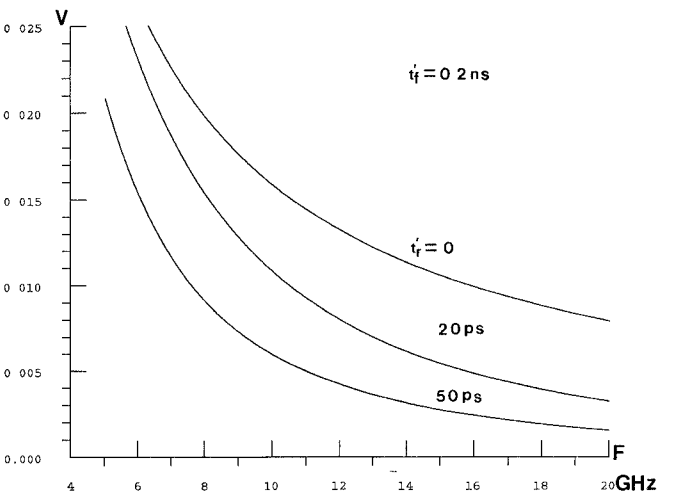


Fig. 3. $|V(\omega)|$ versus $\omega$ for different $t_r'$, $t_f' = 0.2$ ns.

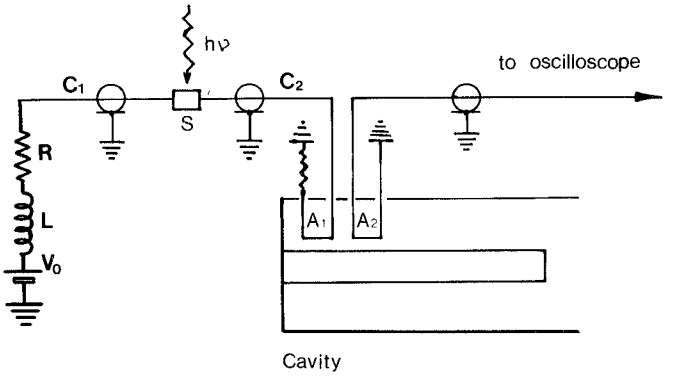


Fig. 4. Schematic of the experimental arrangement. $C_1$ is the coaxial charge line. $C_2$ is the coaxial line, initially uncharged, that connects the photoconductive switch $S$ to the cavity. $A_1$ and $A_2$ are input/output coupling elements.

cause of its long carrier lifetime (1–100 $\mu$s). Unfortunately, it has a low dark resistivity, and thus is prone to thermal runaway. Workers have gotten around the low-voltage hold-off capability of Si by either pulse biasing the PS or operating at low temperature [15], [16]. We have used both GaAs and Si in a scheme where the advantage of GaAs is realized in holding HV dc bias, and the advantage of Si is realized in electrical pulse shaping and cleaning [7]. The penetration depth of optical radiation in semiconductors depends on the wavelength. For HV PS operation, one should use a laser wavelength that results in the deep penetration of photons into the PS. This avoids very high current densities at the surface and thus does not damage the PS. We use radiation at 1.06 $\mu$m, where penetration depth of millimeters in Si and GaAs is realized, instead of 0.532-$\mu$m radiation with penetration depths of microns [17].

## III. Experimental System

A schematic of the experimental arrangement is shown in Fig. 4. Coaxial slotted lines were used as quarter-wave resonant cavities. Specifically, a 25-cm-long HP slotted line cavity, resonating at 300 MHz, and a 9-cm-long home-made cavity, resonating at 1 GHz, were used. These resonant frequencies are for high-$Q$ operation of the cavities. An active–passive mode-locked Nd:YAG laser is used to generate ~1 mJ of 1.06-$\mu$m radiation, with 100 ps pulsewidth and a repetition rate of 1 Hz, to trigger the bulk GaAs PS. The performance of the GaAs PS's were tested, under dc biases of up to 4 kV, with 1.06-$\mu$m laser pulses for several thousand consecutive shots without any observable degradation in performance.

A high-voltage power supply charges the coaxial line $C_1$ to 2.5 kV. The center wire of $C_1$ is joined to that of the coaxial line $C_2$ through the GaAs PS. $C_2$ is connected to the resonant cavity through the input coupling element $A_1$. Coupling element $A_2$ is the output port. $C_1$ and $C_2$ were type RG-58A/U with $Z_0 = 50\ \Omega$. Activating the PS by an optical pulse generates a rectangular (monopolar) electric pulse of width equal to twice the electrical length of $C_1$. The magnitude of the monopolar pulse will be half the dc charged voltage at most, since $C_1$ and $C_2$ have equal characteristic impedances. The monopolar pulse is transmitted through $C_2$ and incident on $A_1$, thus exciting the resonant cavity. The generated microwave pulses are extracted through the output coupling element $A_2$. A 1-ns rise-time storage scope is used to observe the generated pulseforms. A homemade $\pi$ attenuator, with a bandwidth of 1 GHz, is used to reduce the magnitude of the pulses. In Fig. 5 we show a typical monopolar electric pulse ($\simeq$1.25 kV in magnitude and 2 ns in duration) used to excite the cavities. This was measured by connecting $C_2$ to the scope through the attenuator. The limited bandwidth of the attenuator makes it appear inductive to the sharp rise and fall of the pulse. This causes the sharp edges of the monopolar pulse. Two important and useful parameters that control the waveform, and hence the frequency distribution, of the generated microwaves are 1) strength of the coupling provided by $A_1$ and $A_2$, and 2) length of the coaxial line $C_2$ connecting the PS to $A_1$.

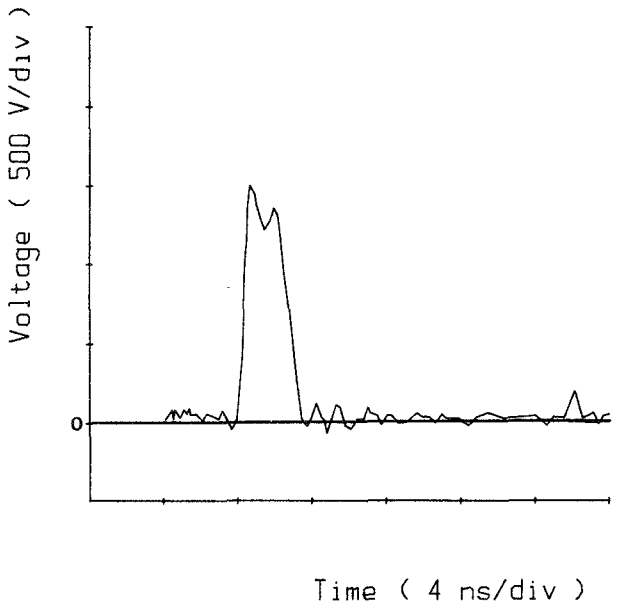


Fig. 5. Typical monopolar electric pulse used to excite the cavities. The pulse is generated by optically triggering the PS.

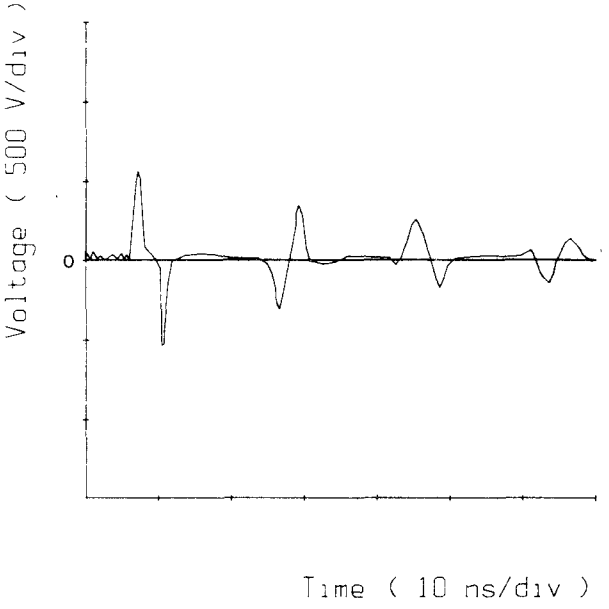


Fig. 6. Successive dipolar microwave pulses generated using the 300-MHz cavity with strongly coupled $A_1$ and $A_2$ and 20-ns-long $C_2$.

The experimental concept has some similarity to previous work by Ristic and Sorensen in the generation of microwaves by spark-gap cavities [18]. However, the differences have significant consequences. For example, PS operation yields picosecond rise times, as compared to the nanosecond rise times in spark-gap operation. Also, PS allows complete synchronization with other optically controlled apparatus, as compared to several nanosecond jitter for spark-gap operation. Furthermore, PS as an external element affords an extra degree of freedom (length of $C_2$) in controlling the generated microwaves.

## IV. Results and Discussion

In Fig. 6 we show the effect of coupling ($A_1$ and $A_2$) and the length of $C_2$. The generated waveform is due to strong coupling at $A_1$ and $A_2$ using the 300-MHz cavity. A strong coupling is obtained by directly connecting the center wire of an input–output coaxial line to the center wire of the coaxial cavity. This kind of coupling loads the cavity heavily. The generated waveform can be explained as follows. Some of the incident voltage pulse on $A_1$ excites the cavity, while some is reflected with a change in sign (since the effective impedance of $A_1$ is less than the characteristic impedance of $C_2$). The reflected pulse suffers an open-circuit reflection at the PS (thus keeping the same sign) and is incident on $A_1$, repeating the above process. The ratio of the magnitudes of successive pulses depends on the coupling strength, and is expected to be constant. The time between successive pulse excitation is expected to be twice the travel time in $C_2$ ($\simeq 20$ ns in this case). The measured ratio of the magnitude of successive pulses is $0.64 \pm 0.03$. The separation between successive pulses is $18.4 \pm 1$ ns in good agreement with the round-trip length of $C_2$. The width of the pulses at the base is $\simeq 6.3 \pm 0.5$ ns. Note that the first dipolar pulse has a peak-to-peak voltage

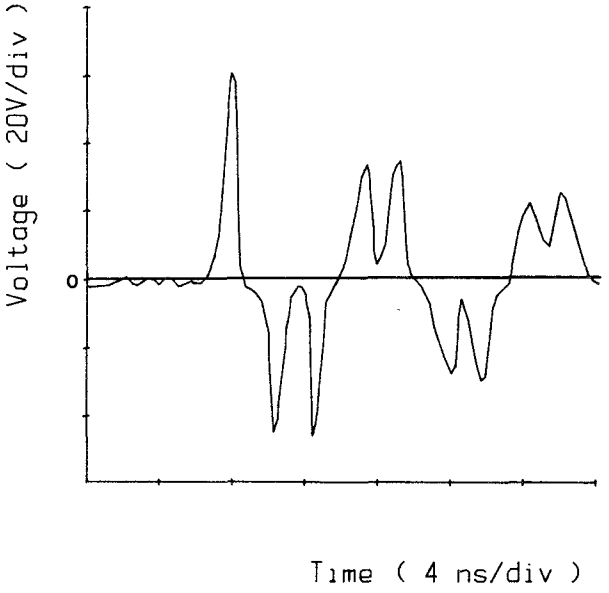


Fig. 7. Successive dipolar microwave pulse generated using the 1-GHz cavity with the intermediate coupling and 5-ns-long $C_2$.

of $\simeq 1.2$ kV, and that the peak power is over 7 kW. The energy conversion efficiency, including the reflected pulses, is over 50 percent.

In Fig. 7 we show the effect of changing the couplings and the length of $C_2$. Intermediate coupling (loop antenna for $A_1$ and strong coupling for $A_2$) is used to excite the 1-GHz cavity, together with a 5-ns-long $C_2$. Note the relatively larger voltages of the reflected pulses due to the weaker coupling at $A_1$.

In Fig. 8 we show the waveform generated by the 1-GHz resonator with strong couplings and $\simeq 0.5$-ns-long $C_2$. Note that the width of the generated single dipolar pulse is larger than the period of the resonance frequency. There are several reasons for this, the most important of which

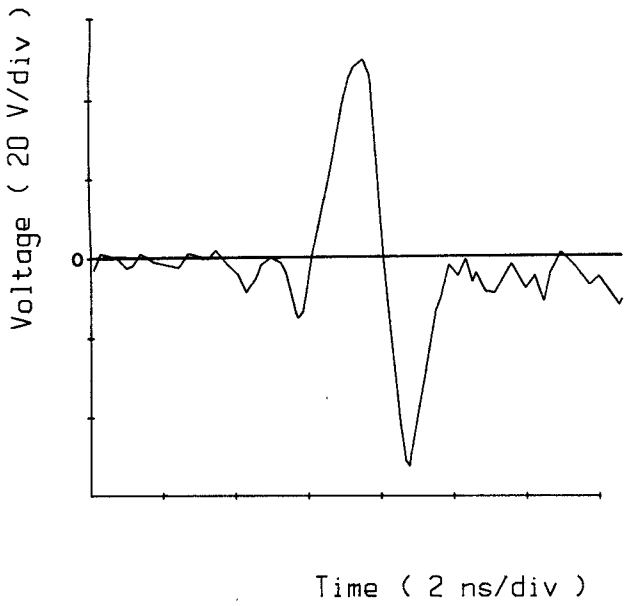


Fig. 8. Single dipolar microwave pulse generated using the 1-GHz cavity with strong coupling and $\simeq 0.5$-ns-long $C_2$.

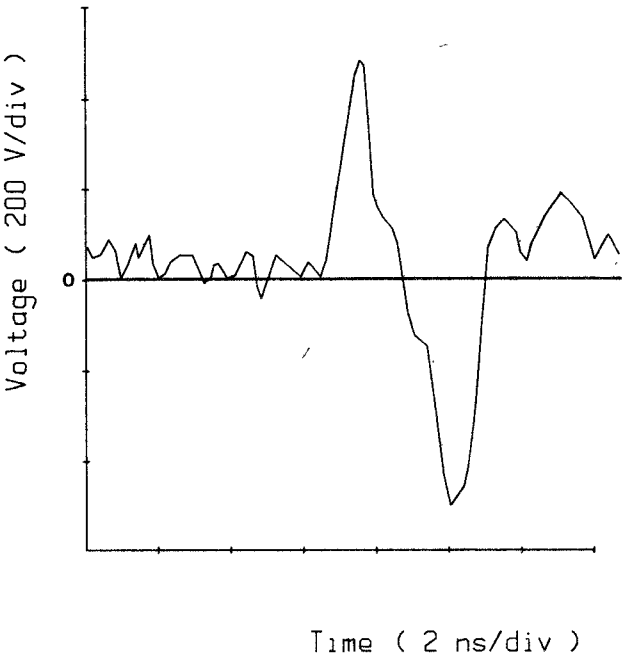


Fig. 9. Single dipolar microwave pulse generated using the 300-MHz cavity with strong coupling and $\simeq 0.5$-ns-long $C_2$.

are: a) the nonzero (0.5 ns) time shift between the (successive) added microwave pulses, b) the loading of the cavity, and c) the finite rise time of the scope. The waveform generated by the 300-MHz cavity in a similar situation is shown in Fig. 9.

The generated microwave forms, Figs. 6–9, are of a wide-band nature. It is important to know the frequency distribution of the power in these waveforms. For simplicity, we assume that the waveforms are rectangular. The Fourier transform of a monopolar rectangular pulse (similar to Fig. 5) is

$$V(\omega) = \sqrt{\frac{2}{\pi}}\,\frac{V_0}{\omega}\sin(\omega t_0/2) \tag{2}$$

where $V_0$ is the height of the pulse and $t_0$ its duration. The Fourier transform for a single dipolar rectangular pulse (similar to Figs. 8 and 9) can be shown to be (see the Appendix)

$$V(\omega) = 2\sqrt{\frac{2}{\pi}}\,\frac{V_0}{\omega}\sin^2(\omega t_0/4) \tag{3}$$

where $t_0$ is the period of the single dipolar pulse. The Fourier transform for a succession of single dipolar rectangle pulses (similar to Figs. 6 and 7) can be shown to be (see the Appendix)

$$V(\omega) = 2\sqrt{\frac{2}{\pi}}\,\frac{V_0}{\omega}\left(\sin^2(\omega t_0/4)\right)\left[1 - a\exp(i\omega t_s)\right]^{-1} \tag{4}$$

where $a$ is the ratio of successive pulse amplitudes ($a$ is negative for out-of-phase successive pulses as in Fig. 6), and $t_s$ is the temporal separation between them. The frequency distribution of the power is proportional to the square of the magnitude of the Fourier transform, i.e., $P(\omega)\alpha|V(\omega)|^2$. In Fig. 10 we show the frequency distribution of the power corresponding to (2)–(4), with the areas

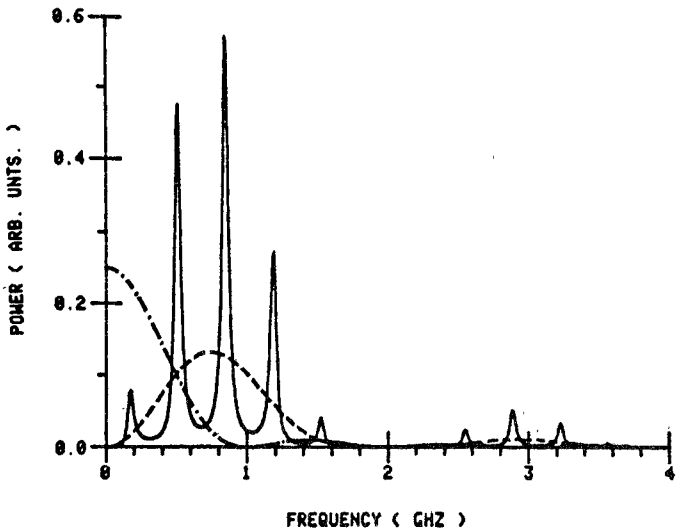


Fig. 10. The power spectrum corresponds to equations (2)–(4). $t_0 = 1$ ns, $t_s = 3$ ns, $a = -0.64$. Dashed–dotted line is for a monopolar pulse. Dashed line is for a dipolar pulse. Solid line is for a multiplexed dipolar pulse. The areas are normalized.

normalized. Note that the monopolar pulse has most of the power in low-frequency components, and that the power in the dipolar pulse peaks at $\sim 0.75/t_0$, i.e., high-frequency components are present with significant power levels at the cost of low-frequency components. Hence, the use of dipolar pulses instead of a monopolar pulse is more efficient for high-power, high-frequency microwave generation. The consequence of multiplexing the dipolar pulse by successive reflections is to squeeze the power into a small number of frequency bands. The center frequencies and the bandwidth are controlled by strength of the couplings ($a$) and the round-trip length of $C_2$ ($t_s$). The bandwidth has narrowed from $\sim 1$ GHz for a single dipolar pulse to

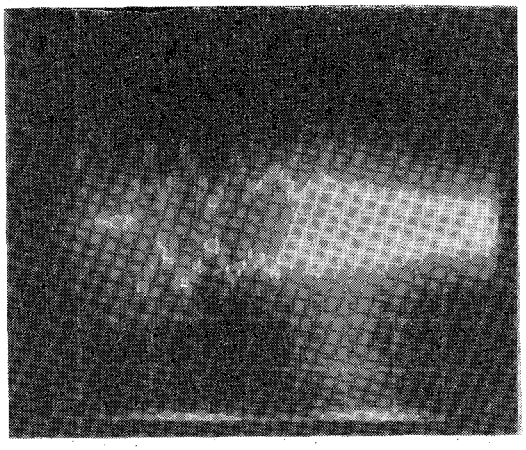

Fig. 11. Microwave generation using the 1-GHz cavity with weak coupling and 5-ns-long $C_2$. (2 V/vertical div., 10 ns/horizontal div.)

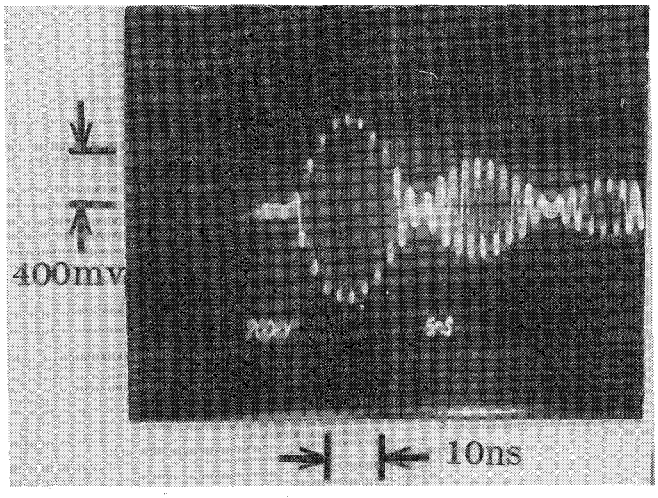


Fig. 12. Microwave generation, using Cr:GaAs and 0.53 mm laser trigger, in a stripline resonant structure biased at 45 V.

~ 50 MHz, in each band, for the multiplexed dipolar pulse. This method of high-power microwave generation, where the frequency can be modulated, lends itself nicely to communication and radar applications. As shown in the Appendix, these observations are not unique to rectangular pulses, but are true in general for any pulse shape that is symmetric about a point.

Finally, a relatively high $Q$ factor is obtained for the cavity when the coupling is weak (loop antennae for $A_1$ and $A_2$). In this case the triggered electrical pulse excites the cavity at its resonant frequency through $A_1$, while $A_2$ allows the extraction of the generated narrow-band microwaves. In Fig. 11 we show the observed waveform for the 1-GHz cavity when $C_2$ is $\simeq 5$ ns long. Note that over 100 mW of 1-GHz RF is generated, with an estimated bandwidth of less than 10 MHz. In this mode of operation (weakly coupled), the cavity acts as a bandpass filter. The modulated envelope is due to beating between the cavity resonant frequency and multiples of the length of $C_2$. The shallow modulation of the envelope is caused by the relatively long lifetime of the PS ( ~ 5 ns). This smears the effective length of $C_2$ and hence affects the beating with the cavity resonant frequency. In Fig. 12 we show the observed waveform when a short lifetime PS (Cr:GaAs) is used. Note the deep modulation of the envelope.

## V. Conclusions

We have shown the versatility of microwave generation through the excitation of a resonant cavity with high-voltage pulses, triggered by a single photoconductive switch. The generated high-power RF waveforms include single wide-band frequencies (dashed line in Fig. 10), multiple narrow-band frequencies (solid line in Fig. 10), and narrow-band cavity resonant frequencies (Figs. 11 and 12). Scaling the power and frequency of generated microwaves to higher values is straightforward. This can be achieved by using a longer PS (so as to hold a higher voltage) and a shorter optical trigger (so as to generate higher frequency microwaves). We are in the process of implementing this. This technique of high-power synchronized microwave generation is expected to find important applications in communication and high-resolution phased-array radar operation.

## Appendix

In this section, we develop the relations between the frequency distribution of the power for monopolar, dipolar, and a series of (i.e., multiplexed) dipolar pulses. On general grounds, we will show that while a monopolar pulse has significant power in low-frequency components, the dipolar pulse will have much smaller power in these frequencies. Instead, the dipolar pulse has significant power in frequency components near the inverse of the cycle period. Furthermore, a series of dipolar pulses will have its power distributed in a number of narrow-band frequencies. The center and width of these bands depend on the envelope of the series and the separation between the individual dipolar pulses.

Monopolar pulses to be considered have the following functional form:

$$V(t) = \begin{cases} V(|t|), & -t_0 \leqslant t \leqslant t_0 \\ 0, & |t| \geqslant t_0. \end{cases} \tag{A1}$$

The Fourier transform gives the frequency components

$$V(\omega) = \frac{1}{\sqrt{2\pi}} \int_{-\infty}^{\infty} V(t) \exp(i\omega t)\, dt$$

$$V(\omega) = V(\omega, t_0).$$

The frequency distribution of the power will then be $P(\omega) \propto |V(\omega)|^2$. We note that $V(\omega \Rightarrow 0) \propto A$ and $P(\omega \Rightarrow 0) \propto A^2$, where $A$ is the amplitude of $V(t)$. This follows from the symmetry of $V(t)$ and $t = 0$ [19]. Indeed, the cosine-like form of $V(\omega \Rightarrow 0)$ for a monopolar pulse (which makes $V(\omega \Rightarrow 0) \propto A$) and the finite power in the pulse (which makes the envelope of $V(\omega)$ decrease monotonically with frequency) lead to an absolute maximum of $V(\omega)$ at $\omega = 0$.

If the axis of symmetry is shifted by $t_s$, then the frequency distribution of the shifted voltage pulse $V_s(\omega, t_0)$

can be related to that for the unshifted voltage pulse $V_{us}(\omega, t_0)$:

$$V_s(\omega, t_0) = \frac{1}{\sqrt{2\pi}} \int_{-\infty}^{\infty} V(|t - t_s|) \exp(i\omega t)\, dt$$
$$= \frac{\exp(i\omega t_s)}{\sqrt{2\pi}} \int_{-\infty}^{\infty} V(|t - t_s|) \cdot \exp[i\omega(t - t_s)]\, d(t - t_s)$$
$$= \frac{\exp(i\omega t_s)}{\sqrt{2\pi}} \int_{-\infty}^{\infty} V(|t'|) \cdot \exp(i\omega t')\, dt'$$

where

$$t' = t - t_s$$

hence

$$V_s(\omega, t_0) = V_{us}(\omega, t_0) \exp(i\omega t_s). \tag{A2}$$

Note that this relation holds for any $V(t)$. Furthermore, changing the width of the pulse from $t_\delta$ to $m_{t\delta}$ yields

$$V(\omega, t_\delta) \Rightarrow V(\omega, mt_\delta). \tag{A3}$$

Next, we consider a dipolar pulse formed from two monopolar pulses. The general form considered is

$$V(t) = \begin{cases} V(|t + t_0/2|), & -t_0 \leqslant t \leqslant 0 \\ -V(|t - t_0/2|), & 0 \leqslant t \leqslant t_0. \\ 0, & |t| \geqslant t_0 \end{cases} \tag{A4}$$

Using (A2) and (A3) one finds the relation between a dipolar pulse $V_{dp}$ and that of a monopolar pulse $V_{mp}$, given by (A1), to be

$$V_{dp}(\omega, t_0) = V_{mp}(\omega, t_0/2)[-e^{i\omega t_0/2} + e^{-i\omega t_0/2}]$$

which can be written as

$$V_{dp}(\omega, t_0) = 2V_{mp}(\omega, t_0/2) \sin(\omega t_0/2) \tag{A5}$$

where a constant phase factor has been suppressed. Note that $V_{dp}(\omega)$ is sine-like for $\omega \Rightarrow 0$. This is to be expected, since (A4) is an odd function about $t = 0$ [19]. Consequently, $V_{dp}(\omega, t_0) = 0$ for $\omega = 0$. Furthermore, the form of $V_{dp}(\omega, t_0)$ and the finite power in the pulse lead to an absolute maximum at $\omega \sim \pi/t_0$.

Finally, we consider a series of pulses given by

$$V(t) = \sum_{n=0}^{\infty} a^n V_{sp}(t - nt_s) \tag{A6}$$

where $|a| < 1$, and $V_{sp}(t - nt_s)$ is the functional form for a single pulse (independent of $n$). Using (A2) one finds that

$$V(\omega) = V_{sp}(\omega) \sum_{n=0}^{\infty} a^n e^{in\omega t_s}$$
$$= V_{sp}(\omega) \sum_{n=0}^{\infty} (ae^{i\omega t_s})^n$$

hence

$$V(\omega) = V_{sp}(\omega) / [1 - ae^{i\omega t_s}]. \tag{A7}$$

Note that the denominator in (A7) modulates the bandwidth inherent in $V_{sp}(\omega)$. The effect of the modulation is to redistribute the power in narrow bands of frequencies within the original bandwidth.

## REFERENCES


[1] G. Mourou, C. V. Stancampiano, and D. Blumenthal, "Picosecond microwave pulse generation," *Appl. Phys. Lett.*, vol. 38, p. 470, 1981.

[2] G. Mourou, C. V. Stancampiano, A. Antonetti, and A. Orszag, "Picosecond microwave pulses generated with a subpicosecond laser-driven semiconductor switch," *Appl. Phys. Lett.*, vol. 39, p. 295, 1981.

[3] R. Heidemann, T. Pfiffer, and D. Jager, "Optoelectronically pulsed slot-line antennas," *Electron. Lett.*, vol. 19, p. 316, 1983.

[4] A. P. DeFonzo, J. Madhuri, and C. Lutz, "Transient response of planar integrated optoelectronic antennas," *Appl. Phys. Lett.*, vol. 50, p. 1155, 1987.

[5] A. Mooradian, "Use of spatial time-division repetition rate multiplication of mode-locked laser pulses to generate microwave radiation from optoelectronic switches," *Appl. Phys. Lett.*, vol. 45, p. 494, 1984.

[6] C. S. Chang, M. J. Rhee, C. H. Lee, A. Rosen, and H. Davis, "Kilovolt sequential waveform generation by picosecond optoelectronic switching in silicon," in *Proc. 1st Topical Meet. on Picosecond Electronics and Optoelectronics*, G. A. Mourou, D. M. Bloom, and C. H. Lee, Eds. New York: Springer–Verlag, 1985.

[7] H. A. Sayadian, S. T. Feng, J. Goldhar, and C. H. Lee, "Generation and forming of ultrashort high voltage pulses" in *Proc. 2nd Topical Meet. on Electronics and Optoelectronics*, C. H. Lee, F. J. Leonberger, F. Capasso, and H. Morkoc, Eds. New York: Springer–Verlag, 1987.

[8] M. G. Li *et al.*, "Direct dc to RF conversion by impulse excitation of a resonant cavity" in *Proc. 1st Topical Meet. on Picosecond Electronics and Optoelectronics*, G. A. Mourou, D. M. Bloom, and C. H. Lee, Eds. New York: Springer–Verlag, 1985.

[9] S. Jayaraman and C. H. Lee, "Observation of two-photon conductivity in GaAs with nanosecond and picosecond light pulses," *Appl. Phys. Lett.*, vol. 20, p. 392, 1972.

[10] D. H. Auston, "Picosecond optoelectronic switching and gating in silicon," *Appl. Phys. Lett.*, vol. 26, p. 101, 1975.

[11] C. H. Lee, Ed., *Picosecond Optoelectronic Devices*. New York: Academic, 1984.

[12] M. Maeda, "An analysis of gap in microstrip transmission lines," *IEEE Trans. Microwave Theory Tech.*, vol. MTT-20, p. 290, 1972.

[13] W. C. Nunnally and R. B. Hammond, "Optoelectronic switch for pulsed power" in *Picosecond Optoelectronic Devices*, C. H. Lee, Ed. New York: Academic, 1984, chap. 12.

[14] D. H. Auston, "Picosecond photoconductors: Physical properties and applications" in *Picosecond Optoelectronic Devices*, C. H. Lee, Ed. New York: Academic, 1984, ch. 5. Also, D. H. Auston, "Impulse response of photoconductors in transmission lines," *IEEE J. Quantum Electron.*, vol. QE-19, p. 639, 1983.

[15] L. Bovino, T. Burke, R. Youmans, M. Weiner, and J. Carter, "Recent advances in optically controlled bulk semiconductor switches" in *Proc. 5th IEEE Pulsed Power Conf.*, 1985 pp. 242–245.

[16] G. Mourou, W. H. Knox, and S. Williamson, "High-power picosecond switching in bulk semiconductors" in *Picosecond Optoelectronic Devices*, C. H. Lee, Ed. New York: Academic, 1984, ch. 7.

[17] C. H. Lee, "Generation of photoinduced carriers" in *Picosecond Optoelectronic Devices*, C. H. Lee, Ed. New York: Academic, 1984, ch. 5, sec. IIb. Also, C. H. Lee, P. S. Mak, and A. P. DeFonzo, "Optical control of millimeter-wave propagation in dielectric waveguides," *IEEE J. Quantum Electron.*, vol. QE-16, p. 277, 1980.

[18] V. M. Ristic and T. P. Sorensen, "Generation of microwave power with a spark-gap cavity," *IEEE Trans. Microwave Theory Tech.*, vol. MTT-26, p. 369, 1978. Also, T. P. Sorensen and V. M. Ristic,

"Rise time and time-dependent spark-gap resistance in nitrogen and helium," *J. Appl. Phys.*, vol. 48, p. 114, 1977.
[19] G. Arfken, *Mathematical Methods for Physicists*, 2nd ed. Academic, 1970, sect. 14.2.

✠

**Hrayr A. Sayadian** (M'87), photograph and biography not available at the time of publication.

✠

**M. G. Li,** photograph and biography not available at the time of publication.

**Chi H. Lee** (M'80–SM'86) received the B.S. degree in electrical engineering from National Taiwan University, Taipei, Taiwan, and the M.S. and Ph.D. degrees in applied physics from Harvard University, Cambridge, MA, in 1959, 1962, and 1968, respectively.

He was with the IBM San Jose Research Laboratory from 1967 to 1968. Since 1968 he has been with the University of Maryland, College Park, where he is now a Professor of Electrical Engineering. His areas of research include picosecond optoelectronics, lasers, optical technique for microwave application, and millimeter-wave devices.

Dr. Lee is a Fellow of the Optical Society of America and a member of the American Physical Society. He also serves as the Chairman of the IEEE MTT-3 technical committee for lightwave technology.